Orientational Distribution of α-Helices in the Colicin B and E1 Channel Domains: A One and Two Dimensional ^{15}N Solid-State NMR Investigation in Uniaxially Aligned Phospholipid Bilayers†

Stephan Lambotte, Pieter Jasperse,‡ and Burkhard Bechinger*

Max-Planck-Institut für Biochemie, Am Klopferspitz 18A, 82152 Martinsried, Germany

Received October 6, 1997; Revised Manuscript Received November 13, 1997⊗

ABSTRACT: Thermolytic fragments of the channel-forming bacterial toxins colicin B and colicin E1 were uniformly labeled with the ^{15}N isotope and reconstituted into uniaxially oriented membranes. These well-aligned samples were investigated by proton-decoupled ^{15}N solid-state NMR spectroscopy at 40.5 and 71.0 MHz. The one dimensional spectra indicate a predominant orientation of the colicin α-helices parallel to the bilayer surface but also the presence of a considerable proportion of peptide bonds that align in a transmembrane direction. The orientational distribution of ^{15}N-labeled amide bonds is nearly identical for colicin B and E1, each a representative of a different group of membrane-active colicins. This comparison indicates common structural features of the water-soluble as well as the bilayer-associated proteins. When the pH is lowered, the orientational distribution of amide vectors exhibits only a small shift from in-plane to transmembrane orientations, in agreement with increased affinity and activity of colicins at acidic conditions. The ^{15}N spectral line shape was independent of the bilayer phospholipid composition (100−75 mol % phosphatidylcholine/0−25 mol % phosphatidylglycerol) or the protein-to-lipid ratio in the range 1.7−12 wt %. Two dimensional separated local field spectroscopy (PISEMA) resolves almost 200 ^{15}N resonances of the colicin B channel protein. Approximately 50 ^{15}N signals resonate in a region characteristic of transmembrane helical residues, in strong support of the previously suggested umbrella conformation of the closed colicin channel.

Colicins are plasmid-encoded bacterial toxins that under stress are released into the environment where they exhibit antibiotic activity. Members of the membrane-active class of these proteins that recognize an outer membrane protein receptor of sensitive *Escherichia coli* cells are transferred through the periplasmic space using the *E. coli* Ton or Tol gene products and, finally, exert their toxic activity at the inner bacterial membrane by means of channel formation (*1*−*3*). Each of these three steps of cytotoxic activity is associated with a distinct functional protein domain. These are, from the protein N- to its C-terminus, the translocation, receptor binding, and channel forming domains (*4*, *5*). A primary sequence comparison of the C-terminal channel domains of the different colicins indicates a close similarity within the colicins A, B, and N, within E1, Ia, and Ib, and to a lesser extent between both groups (*6*) (Figure 1). Although these proteins are very water soluble, they insert into the cytoplasmic membrane where they form voltage-gated membrane channels (*7*−*9*). *In vivo*, the transfer of colicins from the medium to the cytoplasm occurs through interactions with bacterial membrane proteins and at the same time results in an insertion competent state close to the inner membrane surface (*2*, *5*, *10*). The C-terminal domains of colicins have been shown to also insert into bilayers of defined composition and to form voltage-gated channels in black lipid membranes (*11*−*14*). These pores result in the permeation of the bacterial membranes, loss of cytoplasmic ions and ATP, and consecutively cell-death (*15*). It has become evident that the structures and membrane insertion mechanisms of the colicin C-termini closely resemble those of other bacterial toxins as well as eukaryotic proteins. These include, e.g., *Bacillus thuringensis* δ-toxin, as well as the toxins of diphteria, tetanus, and botulinum (*16*). The colicins, therefore, provide interesting model systems to study the structures as well as the biophysical interactions that govern protein insertion, pore formation, and regulated cell killing.

The conformations of the C-terminal fragments of several colicins have been determined in membrane-free environments by X-ray crystallography (*6*, *17*, *18*) as well as multidimensional solution NMR spectroscopy (*19*). The secondary and tertiary folds of these proteins closely resemble each other. They are characterized by 10 α-helices arranged in a three-layered structure (Figure 1). The

† This work was Supported by Deutsche Forschungsgemeinschaft (Grant Be1247).

* Corresponding author: Tel: +49 89 8578-2466. Fax: +49 89 8578-2876. E-mail: bechinge@biochem.mpg.de.

‡Present address: Laboratory of Biochemistry, Wageningen Agricultural University, Dreijenlaan 3, 6703 HA Wageningen, The Netherlands.

⊗ Abstract published in *Advance ACS Abstracts,* December 15, 1997.

[1] Abbreviations: CD, circular dichroism; colicin X-thl, thermolytic fragment of colicin X; DMPC, 1,2-dimyristoyl-*sn*-glycero-3-phosphocholine; FTIR, Fourier transform infrared; NMR, nuclear magnetic resonance; PC, phosphatidylcholine; PG, phosphatidylglycerol; PISEMA, polarization inversion spin exchange at the magic angle; POPC, 1-palmitoyl-2-oleoyl-*sn*-glycero-3-phosphocholine; POPG, 1-palmitoyl-2-oleoyl-*sn*-glycero-3-phosphoglycerol.

S0006-2960(97)02467-7 CCC: $15.00
Published on Web 01/06/1998

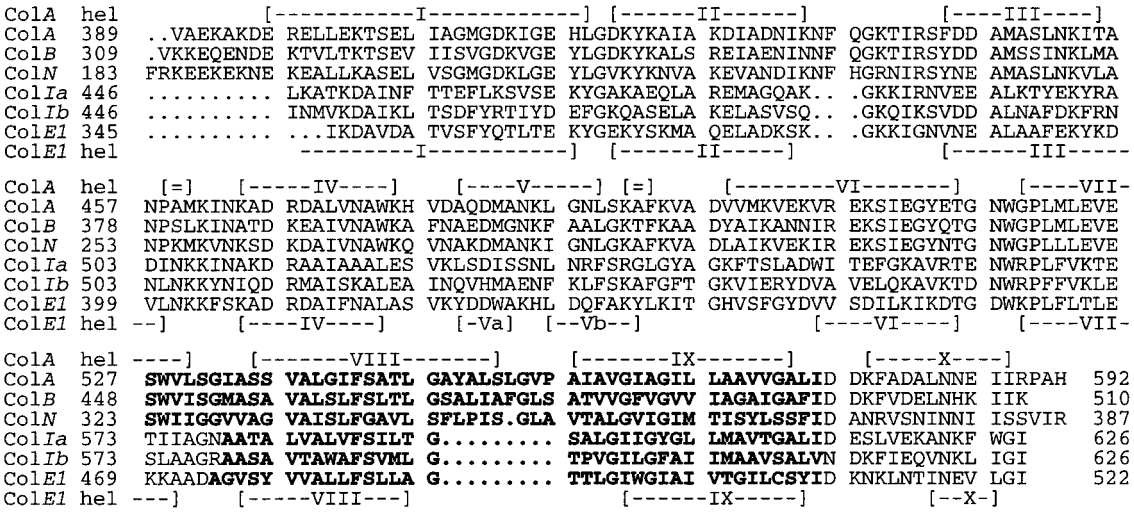

FIGURE 1: Alignment of the carboxy-terminal sequences of several colicins. The numbers represent the amino acid positions in the full-length protein sequence. α-Helical structures of colicin A (*6*) and colicin E1 (*17*) are indicated by a bar above or below the protein sequences, respectively. In colicin A, 3.10 helical structures are indicated by a double bar (=). The extended hydrophobic regions around helices 8 and 9 are shown in bold letters.

hydrophobic core of the soluble colicins consist of a hairpin formed by helices 8 and 9, which is surrounded by amphipathic and hydrophilic regions. The overall high degree of helical secondary structure is preserved when the protein inserts into model membranes (*20*−*22*). The secondary structure, hydrodynamic radius, and protease accessibility indicate that the insertion intermediate forms a molten globule (*23, 24*). An annulus of positively charged residues has been suggested to interact with the negatively charged surface of membranes (*17, 25*), thereby holding the protein in an insertion competent alignment. Low pH helps to open the dense packing of the soluble protein, therefore, acidic phospholipids and pH increase the kinetics of colicin membrane insertion *in vivo* (*15, 26*) and *in vitro* (*13, 27, 28*). In order to match the interfacial properties of lipid bilayers, however, refolding of the tertiary arrangement occurs. The more protease accessible packing of the intermediate, however, is retained in the membrane-bound state of colicins (*29*−*31*). Two models have been suggested to describe the membrane-associated structures of the closed colicin channels (e.g., Figure 1 in ref *30*). First, the umbrella model in which the two hydrophobic helices are arranged in a transmembrane orientation and the amphipathic helices intercalate into the interface (*17, 21, 32*). Second, the pen knife model in which the helices all orient approximately parallel to the surface and form tightly packed structures (*33*). Whereas experimental evidence has been collected in support of the umbrella model for colicin E1 (*5, 31, 34*), experimental data in support of the pen knife model exist for the colicin A/B channel (*9, 30, 33, 35*). The three dimensional structures of the membrane-bound states, however, are unknown. The question, therefore, remains if the two groups of colicins assume different conformations in membrane environments, despite their functional relationship and the similarity of their structures in solution.

Solid-state NMR spectroscopy has proven to provide valuable structural information about proteins when associated with lipid bilayers. Whereas isotropic spectra are recorded when the nuclear anisotropies are averaged in fast rotating samples, the ^{15}N chemical shift and ^{1}H-^{15}N dipolar couplings of proton-decoupled ^{15}N solid-state NMR spectra recorded in uniaxially oriented membranes have been shown to provide information about the alignment of chemical bonds with respect to the bilayer normal (*36*−*38*). Solid-state NMR spectroscopy has been used to analyze the secondary structure of polypeptides when associated with uniaxially oriented membranes (*39, 40*), and to align α-helical domains of labeled polypeptides with respect to the membrane surface (*41, 42*). The ^{15}N chemical shift information, to first order, correlates in a direct manner with the orientation of amide bond NH vectors as well as polypeptide helix axes and has, therefore, proven particularly useful during the analysis of the membrane topology of α-helices (*36, 38*).

Whereas chemical synthesis of polypeptides allows one to incorporate the ^{15}N isotope at selected sites, uniform labeling with isotopes can be more easily achieved when polypeptides are overexpressed and purified by biochemical methods. The recent development of solid-state NMR pulse sequences that efficiently decouple homonuclear ^{1}H−^{1}H interactions (*43, 44*) allow for well-resolved multidimensional solid-state NMR spectra of oriented protein samples. By spreading the resonances in two or more dimensions, each representing an orientationally dependent nuclear interaction, several dozen signals in the amide regions have been resolved by their ^{15}N-^{1}H dipolar coupling as well as their ^{15}N and ^{1}H chemical shift (*45*). Although the large size of the anisotropic nuclear interactions present in immobilized samples requires special consideration, these new solid-state NMR techniques provide spectra that resemble, in many ways, those obtained by NMR spectroscopy of proteins in solution.

In the present work, the thermolytic fragments of colicin E1 and B, each a representative of a colicin group, have been uniformly labeled with ^{15}N by overexpression in *E. coli* cells, purified by biochemical methods and reconstituted into oriented phospholipid bilayers. One dimensional proton-decoupled ^{15}N solid-state NMR spectra have been recorded in order to compare the overall orientational distribution of amide bond NH vectors in bilayer-associated colicin E1 and B. The umbrella model is characterized by a helical hairpin which is oriented parallel to the bilayer normal, therefore, according to this model, at least 20% of the ^{15}N-labeled amides are expected to resonate at ^{15}N chemical shift

frequencies ≥ 180 ppm. These transmembrane helices are absent in the pen knife model; therefore, the chemical shift distribution allows one to differentiate between the two suggested models in a straightforward manner. Furthermore, the effects on the ^{15}N spectral line shape of phospholipid composition and pH have been investigated. High-resolution two dimensional solid-state NMR spectroscopy of selected samples allows one to establish the distribution of α-helical residues parallel to the bilayer normal or in an in-plane alignment in further detail. The results and methods presented in this paper also indicate that the reconstitution and uniaxial alignment of membrane proteins in phospholipid bilayers is possible under nondenaturing conditions.

MATERIALS AND METHODS

Overexpression and purification of thermolytic fragments of colicin E1 and colicin B closely followed the protocols of Cleveland et al. (*32*) and Pressler et al. (*46*), respectively. In particular, the autotrophic strains *E. coli* JM101 bearing the plasmid pColE1::Tn3 M420/516 or pES3 (ColB) (*46*) were used to express colicins in M9 minimal medium containing $^{15}NH_4Cl$ as sole nitrogen source. In order to reconstitute the colicin thermolytic fragments into membranes, the lyophilized proteins were dissolved in water shortly before addition to the appropriate amount of small unilamellar vesicles (50 mg/mL) which had been extruded >10 times through 50 nm membranes. The resulting dispersion was incubated at room temperature for 1 h and concentrated to a final volume of 2−3 mL. The pH was adjusted by adding 0.5% ammonia or 50 mM acetate. This lipid-protein dispersion was evenly spread onto the center of 25 cover glasses (11 × 22 mm). The membranes were slowly dried and equilibrated in 93% relative humidity before the glass plates were stacked on top of each other.

For solid-state NMR measurements, the samples were tightly sealed, inserted into flat coil probe heads (*47*), and introduced into the spectrometer with the bilayer normal parallel to the magnetic field direction. Proton-decoupled ^{15}N NMR spectra were acquired at 9.4 T using a Bruker AMX400 spectrometer with MSL high power cabinet or a home-built NMR spectrometer operating at 16.4 T. At 40.551/400.148 MHz, a cross polarization pulse sequence (*48*, *49*) was applied using the following parameters: mix time 1.6 ms, recycle delay 3 s, acquisition time 6 ms, variable proton B_1 fields of 25−45 kHz, and number of scans typically 8000. For processing, a line broadening of 300 Hz was applied before Fourier transformation. The two dimensional PISEMA solid-state NMR experiments (*43*) were acquired at 70.98/700.38 MHz using B_1-fields of 52 kHz. In order to avoid excessive sample heating the duty cycles were reduced. A total of 128 rows were recorded in t_1 with a dwell time of 39.4 ms. A sine bell function for moderate resolution enhancement as well as an exponential line broadening of 50 Hz were applied to the ^{15}N chemical shift dimension. The ^1H-^{15}N dipolar interaction axis has been corrected by the scaling factor of 0.82 of the PISEMA experiment (*43*). The ^{15}N chemical shifts were calibrated with respect to ^{15}N ammonium sulfate (27 ppm); thus, the scales are given with respect to a liquid NH_3 reference.

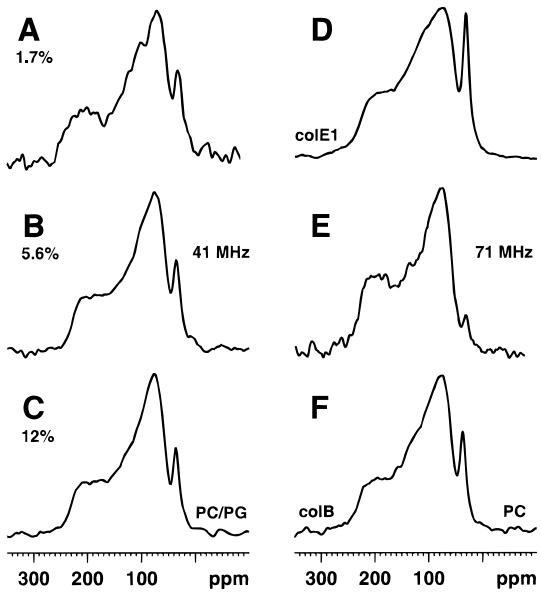

FIGURE 2: Proton decoupled ^{15}N solid-state NMR spectra of thermolytic fragments of colicin B (panels A−C, E, and F) or colicin E1 (panel D) in oriented phospholipid bilayers at neutral pH. (A−C) Concentration dependence of colicin B-thl in POPC/POPG 80:20, pH 7, recorded at 9.4 T: (A) 1.7 wt %; (B) 5.6 wt %; (C) 12 wt %; (E) same sample as used for spectrum B recorded at 16.4 T; (D) 12 wt % colicin E1-thl in POPC membranes, pH 5.8; (F) 12 wt % colicin B-thl in POPC membranes, pH 7.

RESULTS

Colicin B and E1 thermolytic fragments were reconstituted into small unilamellar vesicles, oriented along glass plates and the resulting membranes equilibrated in an atmosphere of 93% relative humidity. The orientational distributions of the peptide bonds of uniformly ^{15}N-labeled colicin B and E1 were determined as a function of protein-to-lipid ratio, lipid composition and pH. Figure 2, panels A−C show the resulting proton decoupled ^{15}N solid-state NMR spectra of colicin B at varying protein concentrations when incorporated into POPC/POPG 80:20 membranes. This concentration of negatively charged lipids is within the optimum range for colicin activity (*50*), and at the same time this lipid composition allows for efficient sample orientation. The amide region of the spectra shown in Figures 2−4 exhibit broad chemical shift anisotropies (240−50 ppm), indicative of proteins that are immobilized by their interactions with the membrane. The thermolytic fragment of colicin B is expected to show resonances from 199 backbone amides, two prolyl bonds (229−32 ppm), as well as the side chains of 20 lysine residues (isotropic shift: ca. 36 ppm), three arginines (74 and 90 ppm), three tryptophanes (84 ppm), 17 asparagines and glutamines (116 ppm), and one histidine (≥170 ppm). The thermolytic fragment of colicin E1 contains 176 residues, including 1P, 24K, 1R, 3W, 10 N+Q, and 2H (Figure 1). Cross polarization of mobile side chains is inefficient, and the corresponding resonances are reduced or absent (*49*). Whereas the diluted samples exhibit a lower signal intensity (Figure 2A), the spectra at all concentrations tested closely resemble each other, indicating that the average orientation of NH vectors with respect to the bilayer normal remains unchanged (Figure 2, panels A−C). This finding is suggestive of a single conformation at all experimental conditions. Due to spectral overlap, the orientational mosaic

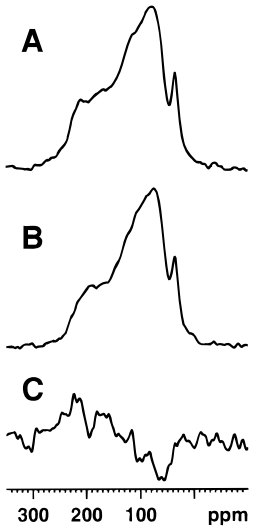

FIGURE 3: Proton decoupled ^{15}N solid state NMR spectra of thermolytic fragments of colicin B in uniaxially oriented bilayers of POPC/POPG 80:20. (A) pH 3.5; (B) pH 7.5; (C) difference spectrum of panel A minus panel B. To make the differences more visible the difference spectrum is shown at larger scale.

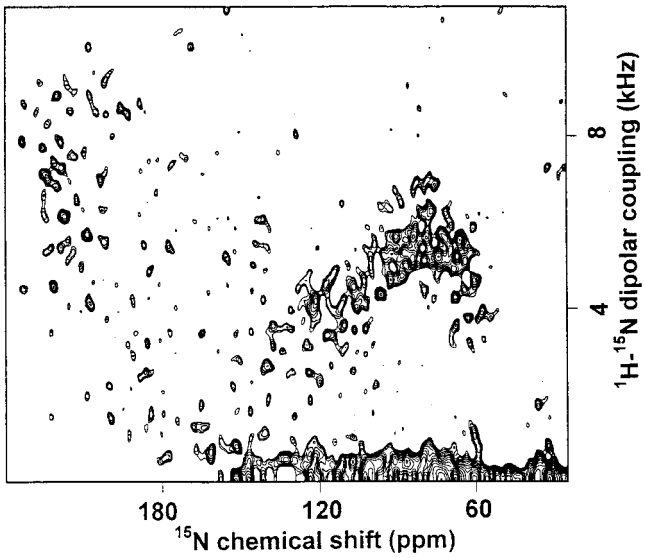

FIGURE 4: Two dimensional 71 MHz PISEMA spectrum of the same sample shown in Figure 2, panels B and E. This spectrum resolves the ^{15}N chemical shifts and the ^1H-^{15}N dipolar interactions of many individual residues (cf. text for details).

spread of individual amide resonances cannot be analyzed from the one dimensional spectra. The narrow line width and the resulting high resolution of single amides in the two dimensional PISEMA spectrum indicates, however, that most of the proteins exhibit uniform alignment with respect to the magnetic field direction (Figure 4). In addition, proton-decoupled Hahn-echo ^{31}P NMR spectra indicate that the oriented liquid crystalline bilayers exhibit an apparent orientational mosaic spread $<15°$ (not shown). When reconstituted into pure phosphatidylcholine membranes the line shapes of the amide regions of the proton-decoupled ^{15}N solid-state NMR spectra of colicin B (Figure 2F) and colicin E1 (Figure 2D) were indistinguishable from those observed of colicin B in PC/PG 80:20 bilayers (Figure 2, panels A−C).

Whereas a ^{15}N chemical shift of >180 ppm (low field) is indicative of helical domains oriented parallel to the bilayer normal, values close to the opposite edge of the chemical shift dispersion are characteristic for in-plane amphipathic helices (*36*). The signal intensities observed in the ^{15}N low-field regions of Figures 2−4, therefore, indicate the presence of a significant number of peptide planes which orient with their NH vector parallel to the bilayer normal. When the NMR spectra were recorded at higher magnetic field strength, the signals from residues in a "transmembrane orientation" appear more separated from the remainder of the spectrum and slightly increased in intensity (Figure 2, panels B and E). The chemical shift dispersion increases in a linear fashion and the uniaxial orientation of the sample becomes apparent also in one dimensional recordings (Figure 2E). High magnetic fields, therefore, provide increased resolution at constant line width (measured in hertz). In addition, the cross polarization efficiency is also dependent on the detailed experimental conditions, including spectrometer electronics, NMR probe heads, and resonance frequencies (*49*). The experimental data obtained at 9.4 or 16.4 T are, therefore, in excellent agreement and result in the same conclusions about the membrane protein structure.

Colicins as well as their channel-forming fragments interact with lipid membranes in a pH-dependent manner (*27, 28*). At low pH, protonation of carboxylate residues enhances the affinity for negatively charged membranes (*25, 50, 51*), destabilizes the packing of the soluble protein (*24*) and, therefore, results in increased insertion kinetics (*52*). Whereas binding of colicins at high pH is reversible (*27, 53*), the proteins more strongly interact with lipid membranes when the pH is lowered indicating an additional hydrophobic contribution (*14, 28, 50, 51*). We, therefore, also compared the orientational distribution of colicin thermolytic fragments at different pH values. Figure 3 indicates that acidification of the sample results in a modest change in the line shape of the resulting ^{15}N NMR spectra. The difference spectrum shows that at most a few percent of the amide intensity shifts from the upfield (<120 ppm) to the downfield region (>150 ppm, Figure 3C).

The colicin B thermolytic fragment in POPC/POPG 80:20 membranes (Figure 2, panels B and E) was investigated in further detail by two dimensional separated local field spectroscopy. This experiment at the same time explores the orientationally dependent ^{15}N chemical shift and the ^1H-^{15}N dipolar coupling. Nutation of the proton spins around the magic angle during the evolution of the heteronuclear dipolar coupling ensures good homonuclear decoupling and narrow lines in the t_1 dimension (*43, 44*). The resulting spectrum is shown as a contour plot in Figure 4. The resolution of nearly 200 resonances indicates that the protein exhibits a uniform alignment with respect to the magnetic field direction. About 50 amides resonate at ^{15}N chemical shifts $\geq$ 180 ppm and exhibit dipolar couplings $\leq$ 20 kHz, indicating an alignment of the NH vector parallel to the bilayer normal. The spectral region between 50 and 130 ppm is much more crowded, in agreement with both models suggested for membrane-bound colicins where the majority of residues are part of amphipathic in-plane helices. This region also contains up to 25 mobile ^{15}N side chain resonances which partly explains the high density of peaks exhibiting zero dipolar coupling.

DISCUSSION

Two models have been suggested to describe the basic structural features of the membrane-bound colicin channel domains. Both models are based on the high content of α-helical conformation found in the crystal structures of colicin A, E1, and Ia (*6*, *17*, *18*). They also include the experimental analysis of CD and FTIR spectra, which indicate a 5−10% increase in helicity upon membrane association (*20*−*22*). In both models, membrane insertion is associated with an inside-out refolding of the compact structure of the colicin thermolytic fragments in solution. As a result, the two hydrophobic helices 8 and 9 (Figure 1) insert into the hydrophobic region of the lipid bilayer, and the amphipathic helices are positioned along the bilayer interface. The major difference between both models is the orientation of the hydrophobic hairpin. Whereas experimental evidence suggests that the colicin E1 helices assume a transmembrane orientation (*5*, *31*, *34*), the colicin A hydrophobic region has been shown to closely associate with the amphipathic in-plane helices (*9*, *30*, *33*, *35*). The possibility remains that, despite the close structural and functional similarities, the two colicin groups assume a different membrane-bound conformation. A comparison of the primary structures of the channel-forming colicin domains (Figure 1) reveals some small differences between the colicin A/B/N and E1/Ia/Ib groups. Most notably, the hydrophobic region comprising helices 8 and 9 is considerably shorter in colicin E1 when compared to colicin A or B (Figure 1). The hydrophobic stretch of colicin A/B consists of 49 residues and seems well suited to span the membrane twice in an α-helical conformation. The deletion of nine residues in colicin E1, however, reduces the hydrophobic length sufficiently to place charged residues into the hydrophobic bilayer region when an α-helical hairpin conformation is assumed. In contrast to the experimental evidence, these theoretical considerations, therefore, suggest a higher tendency of the colicin A hydrophobic hairpin to cross the lipid bilayer when compared to colicin E1. The energetic penalty for placing some of the EKK(468−470), D473, and DKNK-(509−512) residues close to the bilayer interface may be relieved by protein counter charges (*54*), or by snorkeling of the asparatate and lysine side chains into the hydrophilic region (*34*). Alternatively, the hydrophobic thickness of the colicin E1 hairpin and the lipid bilayer may be matched by an elongated 3.10 helical arrangement or by local bilayer deformations.

The one and two dimensional solid-state NMR spectra presented in Figures 2−4 indicate that approximately 50 amide resonances of the thermolytic fragment of colicin B exhibit ^{15}N chemical shift resonances of ≥180 ppm, i.e., in a region that is characteristic of helical residues that assume a transmembrane orientation. When the ^{15}N chemical shift spectra of the thermolytic fragments of colicin E1 and B are compared, the line shapes are of striking similarity, indicating that the orientational distribution of the peptide bond NH vectors is comparable. An independently performed solid-state NMR investigation of the thermolytic fragment of colicin E1 (176 residues) indicates that about 40 residues align in a transmembrane fashion (*55*). Although the resonances of these spectra cannot be unambiguously assigned at the present stage, hydrophobicity analysis (*56*), site-directed mutagenesis in combination with measurements of the cytotoxicity of the resulting protein product (*34*), and proteolysis experiments (*29*) all suggest that most of the amides of colicin B and E1 that resonate at ^{15}N chemical shifts of ≥180 ppm belong to a transmembrane helical hairpin formed by helices 8 and 9. The similarity of the solid-state NMR spectra of colicin B and E1 in their bilayer-associated state reflect their close structural and functional relationships (Figure 2, panels D and F) as well as the close resemblance of the colicin x-ray structures in the absence of membranes (*6*, *17*) and a high degree of primary sequence similarity (ca. 35%).

A multitude of experimental findings with colicin A shows, however, that the hydrophobic hairpin remains associated with the amphipathic helices close to the bilayer interface. These include fluorescence transfer energy measurements, which indicate that the distance increases between helices are insufficient to account for the conformational changes suggested by the umbrella model (*33*). In addition neutron diffraction experiments show a predominant increase in density along the bilayer interface upon colicin membrane interaction (*35*), and protease digestion experiments indicate that the hydrophobic region of colicin A remains accessible to proteases added to the outside of small unilamellar DMPG vesicles, but not when the proteases are trapped inside (*30*).

In order to resolve the seeming discrepancy between the structural findings, one could argue that colicin A and B assume very different conformations in the membrane-associated state. The primary sequence similarity, however, is very high throughout the whole sequence of the channel-forming domains of colicin A and B (71% in average). Therefore, large conformational differences are not expected, in particular when considering that the much less related colicins E1 and B exhibit striking structural similarities in solid-state NMR investigations (cf. above). The use of different membrane systems has been shown to have a profound effect on the association of polypeptides with phospholipid membranes. Whereas in previous investigations, the interactions of colicin A with negatively charged membranes of phosphatidylglycerol have been studied, the negative surface charge density did not exceed 25 mol % in this work. Although the presence of a negative surface charge density is important for the functional association, alignment, and insertion into membranes, a delicate equilibrium exists between hydrophobic and electrostatic interactions (*25*, *51*). It has been shown for colicin E1 that the activity of this protein drops sharply when the membrane contains more than 50 mol % acidic phospholipids (*50*). Colicin binding can be reversed at elevated pH (*27*, *53*), and the tip of a biotinilated hydrophobic hairpin of the closed colicin Ia channel is accessible to streptavidin from both the *cis* and the *trans* side (*57*). The soluble and intermediate colicin conformations, therefore, are in equilibrium with each other. These equilibria are shifted by the bilayer lipid composition, pH, lipid packing, and interactions with other proteins or colicin domains. The positioning of the helical hairpin is particularly labile as the putative interhelical turn does not contain charged residues that would anchor the sequence at the opposite membrane surface (Figure 1). The possibility also exists that, in the presence of high phosphatidylglycerol concentrations, the transition from the soluble colicin insertion intermediate to the "closed channel"

is slowed sufficiently to allow for the observation of membrane-bound insertion intermediates, including the pen knife conformation. In contrast, the NMR samples used in this study are incubated for several days, and the proteins forced into close proximity of the membranes during the preparation process. In these samples, the colicin molecules have reached their low-energy conformation, and under the experimental conditions of this study, the observation of a kinetically trapped insertion intermediate seems unlikely. The data presented, therefore, support the presence of two transmembrane helices in both the colicin E1 and the colicin A/B groups once a thermodynamic equilibrium in moderately charged phospholipid membranes has been reached.

When the pH of the medium is lowered, a modest transition of amide NH vectors from an "in-plane alignment" into a "transmembrane orientation" is observed. Amphipathic polypeptides have previously been shown to reorient from an in-plane alignment into a transmembrane configuration when charged amino acids are neutralized (*58*). The balance of electrostatic, hydrophobic, and polar interactions determines the midpoint of these transitions. Whereas the solid-state ^{15}N chemical shift provides information about the orientation of α-helices with respect to the bilayer surface (*36*,*38*), ^{2}H and ^{31}P solid-state NMR investigations of deuterated phospholipid dispersions indicate significant changes of membrane association and bilayer penetration depth when the pH is lowered (*59*). Protonation of asparatate and glutamate residues neighboring the hydrophobic region of colicin B may cause the extension of the transmembrane helices (Figure 1), but membrane insertion and reorientation of other regions is equally well possible.

The orientationally dependent chemical shift and dipolar interactions are well resolved in the spectrum shown in Figure 4 and contain the information necessary for the calculation of protein conformations (*39, 40*). Once methods for the assignment of most ^{15}N resonances are available, the complete structure determination of bilayer-associated proteins will, therefore, be possible.

ACKNOWLEDGMENT

We are grateful to Volkmar Braun and Wayne Hubbel for providing the colicin constructs. Jutta Luig and Mechthild Raude were of great technical help during protein purification. We are grateful to Kathy Valentine and Stanley J. Opella for their help and for providing spectrometer time at the 700 MHz instrument of the *NIH resource for solid-state NMR of proteins*. We are thankful to Rolf Kinne for his support during the initial stages of this project.

REFERENCES

1. Slatin, S. L. (1988) *Int. J. Biochem. 20*, 737.
2. Lakey, J. H., van der Groot, F. G., and Pattus, F. (1994) *Toxicology 87*, 85.
3. Stroud, R. (1995) *Curr. Opin. Struct. Biol. 5*, 514.
4. Lazdunski, C. J., Baty, D., Geli, V., Cavard, D., Morlon, J., Lloubes, R., Howard, S. P., Knibiehler, M., Chartier, M., and Varenne, S. (1988) *Biochem. Biophys. Acta 947*, 445.
5. Cramer, W. A., Heymann, J. B., Schendel, S. L., Deriy, B. N., Cohen, F. S., Elkins, P. A., and Stauffacher, C. V. (1995) *Ann. Rev. Biophy. Biomol. Struct. 24*, 611.
6. Parker, M. W., Postma, J. P., Pattus, F., Tucker, A. D., and Tsernoglou, D. (1992) *J. Mol. Biol. 224*, 639.
7. Bourdineaud, J. P., Boulanger, P., Lazdunski, C., and Letellier, L. (1990) *Proc. Natl. Acad. Sci. U.S.A. 87*, 1037.
8. Benedetti, H., Lloubes, R., Lazdunski, C., and Letellier, L. (1992) *EMBO J. 11*, 441.
9. Duche, D., Parker, M. W., Gonzalez-Manas, J. M., Pattus, F., and Baty, D. (1994) *J. Biol. Chem. 269*, 6332.
10. Duche, D., Baty, D., Chartier, M., and Letellier, L. (1994) *J. Biol. Chem. 269*, 24820.
11. Raymond, L., Slatin, S. L., and Finkelstein, A. (1985) *J. Membr. Biol. 84*, 173.
12. Collarini, M., Amblard, G., Lazdunski, C., and Pattus, F. (1987) *Eur. Biophys. J. 14*, 147.
13. Bullock, J. O., Armstrong, S. K., Shear, J. L., Lies, D. P., and McIntosh, M. A. (1990) *J. Membr. Biol. 114*, 79.
14. Levinthal, F., Todd, A. P., Hubbell, W. L., and Levinthal, C. (1991) *Proteins 11*, 254.
15. Letellier, L. (1992) *Biochem. Biophys. Acta 1101*, 218.
16. Parker, M. W., Tucker, A. D., Tsernoglou, D., and Pattus, F. (1990) *Trends Biochem. Sci. 15*, 126.
17. Elkins, P., Bunker, A., Cramer, W. A., and Stauffacher, C. V. (1997) *Structure 5*, 443.
18. Wiener, M., Freymann, D., Ghosh, P., and Stroud, R. M. (1997) *Nature 385*, 461.
19. Wormald, M. R., Merrill, A. R., Cramer, W. A., and Williams, R. J. (1990) *Eur. J. Biochem. 191*, 155.
20. Goormaghtigh, E., Vigneron, L., Knibiehler, M., Lazdunski, C., and Ruysschaert, J. M. (1991) *Eur. J. Biochem. 202*, 1299.
21. Lakey, J. H., Massotte, D., Heitz, F., Dasseux, J. L., Faucon, J. F., Parker, M. W., and Pattus, F. (1991) *Eur. J. Biochem. 196*, 599.
22. Rath, P., Bousche, O., Merrill, A. R., Cramer, W. A., and Rothschild, K. J. (1991) *Biophys. J. 59*, 516.
23. van der Goot, F. G., Gonzalez-Manas, J. M., Lakey, J. H., and Pattus, F. (1991) *Nature 354*, 408.
24. Steer, B. A., and Merrill, A. R. (1997) *Biochem. 36*, 3037.
25. Lakey, J. H., Parker, M. W., Gonzalez-Manas, J. M., Duche, D., Vriend, G., Baty, D., and Pattus, F. (1994) *Eur. J. Biochem. 220*, 155.
26. van der Goot, F. G., Didat, N., Pattus, F., Dowhan, W., and Letellier, L. (1993) *Eur. J. Biochem. 213*, 217.
27. Davidson, V. L., Brunden, K. R., and Cramer, W. A. (1985) *Proc. Natl. Acad. Sci. U.S.A. 82*, 1386.
28. Evans, L. J., Goble, M. L., Hales, K. A., and Lakey, J. H. (1996) *Biochemistry 35*, 13180.
29. Zhang, Y. L., and Cramer, W. A. (1992) *Protein Sci. 1*, 1666.
30. Massotte, D., Yamamoto, M., Scianimanico, S., Sorokine, O., van Dorsselaer, A., Nakatani, Y., Ourisson, G., and Pattus, F. (1993) *Biochemistry 32*, 13787.
31. Palmer, L. R., and Merrill, A. R. (1994) *J. Biol. Chem. 269*, 4187.
32. Cleveland, M. V., Slatin, S., Finkelstein, A., and Levinthal, C. (1983) *Proc. Natl. Acad. Sci. U.S.A. 80*, 3706.
33. Lakey, J. H., Duche, D., Gonzalez-Manas, J. M., Baty, D., and Pattus, F. (1993) *J. Mol. Biol. 230*, 1055.
34. Song, H. Y., Cohen, F. S., and Cramer, W. A. (1991) *J. Bacteriol. 173*, 2927.
35. Jeanteur, D., Pattus, F., and Timmins, P. A. (1994) *J. Mol. Biol. 235*, 898.
36. Bechinger, B., Kim, Y., Chirlian, L. E., Gesell, J., Neumann, J.-M., Montal, M., Tomich, J., Zasloff, M., and Opella, S. J. (1991) *J. Biomol. NMR 1*, 167.
37. Cross, T. A., and Opella, S. J. (1994) *Curr. Opin. Struct. Biol. 4*, 574.
38. Bechinger, B., Gierasch, L. M., Montal, M., Zasloff, M., and Opella, S. J. (1996) *Solid-State NMR 7*, 185.
39. Bechinger, B., Zasloff, M., and Opella, S. J. (1993) *Protein Sci. 2*, 2077.
40. Ketchem R. K., Hu W., and Cross T. A. (1993) *Science 262*, 1457.
41. Smith, R., Separovic, F., Milne, T. J., Whittaker, A., Bennett, F. M., Cornell, B. A., and Makriyannis, A. (1994) *J. Mol. Biol. 241*, 456.
42. North, C. L., Barranger-Mathys, M., and Cafiso, D. S. (1995) *Biophys. J. 69*, 2392.

43. Wu, C. H., Ramamoorthy, A., and Opella, S. J. (1994) *J. Magn. Reson. 109*, 270.
44. Ramamoorthy, A., Wu, C. H., and Opella, S. J. (1995) *J. Magn. Reson. B 107*, 88.
45. Marassi, F. M., Ramamoorthy, A., and Opella, S. J. (1997) *Proc. Natl. Acad. Sci. U.S.A.* 94.8551.
46. Pressler, U., Braun, V., Wittmann-Liebold, B., and Benz, R. (1986) *J. Biol. Chem. 261*, 2654.
47. Bechinger, B., and Opella, S. J. (1991) *J. Magn. Reson. 95*, 585.
48. Pines, A., Gibby, M. G., and Waugh, J. S. (1973) *J. Chem. Phys. 59*, 569.
49. Levitt, M. H., Suter, D., and Ernst, R. R. (1986) *J. Chem. Phys. 84*, 4243.
50. Zakharov, S. D., Heymann, J. B., Zhang, Y. L., and Cramer, W. A. (1996) *Biophys. J. 70*, 2774.
51. Heymann, J. B., Zakharov, S. D., Zhang, Y. L., and Cramer, W. A. (1996) *Biochem. 35*, 2717.
52. Gullion, T., and Schaefer, J. (1989) *J. Magn. Res. B 81*, 196.
53. Xu, S., Cramer, W. A., Peterson, A. A., Hermodson, M., and Montecucco, C. (1988) *Proc. Natl. Acad. Sci. U.S.A. 85*, 7531.
54. Honig, B. H., and Hubbell, W. L. (1984) *Proc. Natl. Acad. Sci. U.S.A. 81*, 5412.
55. Marassi, F. M., Almeida, F. C. L., Ramamoorthy, A., Kim, Y., Zasloff, M., Schendel, S. L., Cramer, W. A., and Opella, S. J. (1996) *Biophys. J. 70*, SU397.
56. Shiver, J. W., Peterson, A. A., Widger, W. R., Furbacher, P. N., and Cramer, W. A. (1989) *Methods Enzymol. 172*, 439.
57. Kienker, P. K., Qiu, X., Slatin, S. L., Finkelstein, A., and Jakes, K. S. (1997) *J. Membr. Biol. 157*, 27.
58. Bechinger, B. (1996) *J. Mol. Biol. 263*, 768.
59. Geli, V., Koorengevel, M. C., Demel, R. A., Lazdunski, C., and Killian, J. A. (1992) *Biochemistry 31*, 11089.

BI9724671